PREPARATIVE ELECTROPHORESIS IN LIQUID COLUMNS STABILIZED BY ELECTROMAGNETIC ROTATION*

II. ARTIFACTS, STABILITY AND RESOLUTION

ALEXANDER KOLIN
Department of Biophysics and Nuclear Medicine, University of California, Los Angeles, Calif. (U.S.A.)
(Received July 1st, 1966)

We shall now consider to what extent the ideal conditions presupposed in the preceding discussion[1] can be realized in practice and will examine the disturbances which can arise as a result of excessive deviations from ideal conditions.

The problem of collection of separated fractions over a prolonged period of time has a remote resemblance to the problem of aiming long-range artillery projectiles. A given ion species escaping from the injector IN** is intended to "hit" an inlet tube of the collector after describing several helical turns about the pair of co-axial magnets. This ionic component must persist in entering the same collector tube throughout the duration of a long separation run. Deviations large enough to inject this component into a neighboring collector tube could lead to re-mixing of separated components and must, therefore, be avoided. It is thus clear that all parameters which determine the pitch of the helical ion paths must be maintained as constant as possible.

CONTROL OF CURRENT AND TEMPERATURE

The constancy of the electrophoretic current is insured within 0.1 % by the use of a constant current power supply (Electronic Measurements Co., Model C 636). This alone is, however, not sufficient, since the potential gradient (and, hence, the pitch of the helix) can change at constant current if the electrical conductivity of the solution is altered. It is, therefore, essential to avoid conductivity changes in buffer solution in the separation cell by perfusing the electrode compartments with fresh buffer solution at a sufficiently rapid rate to minimize the effects of electrolysis upon the composition of the electrolytes in these compartments.

Since the electrical conductivity depends on the temperature of the solution, stabilization of thermal conditions in the separation cell is essential before beginning a separation run. The local temperatures as well as the temperature gradients within the annular electrophoretic column must remain constant to avoid shifts of the separation pattern relative to the collector tubes. The temperature in the annulus is not uniform. There are relatively small axial temperature gradients and a very steep radial one. As a result of these temperature gradients, there will be gradients of

* The work has been supported by a grant from the Office of Naval Research.
** See Part I (ref. 1) for key to abbreviations concerning the parts of the apparatus.

viscosity which will affect the velocity distribution and electrical conductivity gradients which will affect the distribution of electrical current density in the annulus. There will, however, be no transverse variation of the potential gradient in the annulus arising from such conductivity gradients. The effects of the temperature gradients upon the helical paths of the ions will be neglected in this paper. The temperature equilibrium is normally achieved within 5 to 10 min.

It is not necessary to maintain the buffer supply in the Mariotte bottle at the temperature of the cooling water which circulates on the inside and outside of the annular electrophoretic column as shown schematically in Fig. 4*. It is sufficient to maintain it constant, for instance, at room temperature. The temperature constancy of the buffer solution in the fine tubing conveying the buffer from the Mariotte bottle to the buffer compartments of the electrophoretic separator and from the collector to the test tubes, as shown in Figs. 3 and 4*, is of particular importance since viscosity fluctuations due to temperature variations will give rise to fluctuations in the pitch of the helical ionic path and, hence, to intermixing of the separated fractions in the collecting test tubes T, T... of Fig. 3*. If the room temperature fluctuates excessively, it is advisable to enclose the above mentioned bundles of polyvinyl chloride tubes in tygon tubing of wider diameter which is to serve as a cooling jacket (not shown in Figs. 3 and 4* to avoid overloading the diagrams). The ends of this outer tube are sealed around the inner tubes (which convey the buffer) with "Teets Denture Material". Side tubes are cemented at either end of the tygon tubing so as to permit circulation of cold water pumped by means of the "cooling water pump" of Fig. 4* through the tygon tubing. In this fashion one insures adequate cooling of the enclosed buffer supply line originating at the manifold MF (Fig. 3)* and of the bundle of collector tubes originating at the collector C of Fig. 3*.

To improve thermal stability, the buffer solution in the buffer compartments B_1 and B_2 can be cooled by insertion of a copper coil or of a different type of heat exchanger into each of them. The heat exchangers are perfused by the cooling fluid from the "cooling water pump" of Fig. 4*. The heat exchanger should be painted with an insulating lacquer such as the one used for coating the injector tube (see above). It should be completely submerged to avoid condensation of atmospheric water vapor on it which would flow into the buffer and dilute it.

If the current density is kept low enough (10–20 mA/cm^2) in buffers of resistivities below 1400 ohm-cm, one may operate conveniently by leaving the buffer solution in the buffer chambers and the water in the cooling water reservoir at room temperature. The sharpest streaks and the most stable collection patterns are obtained, however, by using an ice-water mixture in the coolant reservoir. At room temperature the concentration of the Hydrion buffer tablets normally used was 1 tablet per 1.5 l of water. With ice cooling, in view of the drop in the buffer conductivity, a concentration of 1 tablet per liter of water was used.

Satisfactory operation, unaffected by drift, can be obtained without readjustment for periods in the order of an hour in a thermostatically controlled room using water at room temperature as a coolant. With ice-water coolant no drifts have been observed in operations extended over many hours.

Typical steady-state temperature values at specified locations within the annu-

* Ref. 1 (Part I of this series).

lus in typical performances using pH 10 Hydrion buffer tablets at a concentration of one tablet per liter are shown in Table I. Temperature determinations were made with a miniature thermistor probe (Yellow Springs Instrument Company Model 43 TD) whose tip was successively placed at four different locations along the electrophoretic column specified in Table I. Due to flexibility of the thermistor probe and the impossibility of centering it with great precision within the transverse temperature gradient in the annulus, the data given in Table I are to be considered as rough approximations. They are sufficient, however, to show that there is no danger of overheating the injected substances under conditions of normal operation.

TABLE I

Location of thermistor probe	*Current (mA)*	*Axial flow (mm/sec)*	*Room temp. = coolant temp. (°C)*	*Buffer temp. in annulus (°C)*
2 mm beyond point of buffer entry into the annulus	40	0.75	23.5	26.2
	20	0.75	23.5	24.4
At the injector	40	0.75	23.5	25.5
	20	0.75	23.5	23.5
Midway between injector and downstream end of electrophoretic column	40	0.75	23.5	27.0
	20	0.75	23.5	24.2
2 mm ahead of the downstream end of the annulus	40	0.75	23.5	27.7
	20	0.75	23.5	24.4

SOME FAVORABLE COMPENSATING FACTORS

The degree of stability of the separation pattern achieved in the absence of elaborate temperature controls seems at first glance surprising. It is reasonable to expect some fluctuation in temperature within the annulus since no special precautions are taken to stabilize the pumping rate of the coolant. The temperature of the fluid within the annulus is determined by an equilibrium between the heat generated by the current in the annulus and the heat removed by the circulating coolant. The local temperature values determine the local values of fluid viscosity, electrical conductivity and electrophoretic mobility. Conceivably, such temperature variations could cause pronounced fluctuations of the helical pitch of the ion paths. On closer consideration, however, it is realized that a high degree of temperature sensitivity is not to be expected because of certain mutually compensating factors.

To begin with, let us consider the spiral path of an electrically neutral particle species resulting from a combination of two mutually perpendicular flows: (1) an axial flow and (2) a tangential flow which is due to rotation of the fluid in the annulus. We shall use the approximation of a parabolic velocity profile[2,3] for both flows (an approximation which improves as the ratio R_i/h of the radius of the inner cylinder (R_i) to the difference $h = R_a - R_i$ between the radii of the outer (R_a) and inner (R_i) cylinder increases). In accordance with previously adopted notation[2] we designate by z the radial distance of a point from the inner cylinder, by h the value of z at the outer

cylinder surface, by u_x and u_y the tangential and axial flow velocities, respectively, and by $\mathrm{d}p/\mathrm{d}x$ and $\mathrm{d}p/\mathrm{d}y$ the tangential and axial forces per unit volume, where $\vec{f} = -\mathrm{d}p/\mathrm{d}x = [\vec{J} \times \vec{B}]$, $\vec{J}$ being measured in abampers/cm^2, $\vec{B}$ in gauss and $\vec{f}$ in dynes.

As previously shown[2,3], the tangential and axial velocity distributions are given by the following expressions:

$$u_x = (1/2\eta)z(z - h)\,\mathrm{d}p/\mathrm{d}x \tag{1}$$

and:

$$u_y = (1/2\eta)z(z - h)\,\mathrm{d}p/\mathrm{d}y \tag{2}$$

(where η is the viscosity of the liquid).

The helical slope is determined by the velocity ratio:

$$\frac{u_y}{u_x} = \frac{\mathrm{d}p}{\mathrm{d}y} \Big/ \frac{\mathrm{d}p}{\mathrm{d}x}. \tag{3}$$

The viscosity of the fluid (η) cancels out as eqn. (3) is obtained from eqns. (1) and (2). One sees thus that variations in temperature which alter the viscosity will have no effect on the pitch of the helical path which results from a combination of axial flow with electromagnetic rotation. Another important consequence of eqn. (3), not related to temperature effects, will be considered below (see passage following eqn. 15).

We shall now consider the temperature effect upon the electrophoretic velocity of an ion moving through an electrolyte solution in a cylindrical buffer column which is traversed by a current which is maintained invariant by a constant-current power supply. We shall assume that the ion under consideration as well as the ions of the electrolyte obey Stokes' law:

$$f = Eze = 6\pi\eta v a \tag{4}$$

(where f is the force propelling the ions of valence z in an electric field E; e is the elementary charge; η is the viscosity of the fluid; v is the ion velocity and a is the radius of the ion which is assumed to be spherical). We can write then for the mobility U of the ion (where $U = v/E$):

$$U = (ze)/(6\pi\eta a) = K/\eta. \tag{5}$$

The conductivity σ of the electrolyte can be expressed in terms of the ionic mobilities as follows[5]:

$$\sigma = z_+N_+U_+ + z_-N_-U_-, \tag{6}$$

where the + and — signs refer to the positive and negative ions, respectively, and N stands for the number of ions per cm^3.

Expressing the ion mobilities U_+ and U_- according to eqn. (5), we get:

$$U_+ = K'_+/\eta \text{ and } U_- = K'_-/\eta, \tag{7}$$

where K_+' and K_-' are constants depending on the valences and radii of the positive and negative ions of the electrolyte, respectively. We obtain thus for σ from eqns. (6) and (7):

$$\sigma = (z_+N_+K'_+ + z_-N_-K'_-)\frac{1}{\eta} = \frac{K''}{\eta} \tag{8}$$

The potential gradient which determines the electrophoretic velocity of a charged particle in the apparatus is given by:

$$d\varphi/dy = J/\sigma = (J/K'')\eta \tag{9}$$

The velocity of a given electrophoretic particle of mobility U in the field $d\varphi/dy$ is thus according to the preceding equations:

$$v_y = (d\varphi/dy)U = (d\varphi/dy)\,(K'/\eta) = (J/K'')\eta\cdot\frac{K'}{\eta} = J\frac{K'}{K''} \tag{10}$$

We see thus that, due to cancellation of viscosity terms in eqn. (10), the velocity of a charged particle in an electrophoretic column should remain at least approximately independent of thermally produced viscosity variations which would affect in similar fashion the mobilities of the electrophoretic particles and those of the conductivity determining electrolyte ions in the migration column. This independence of the axial electrophoretic ion velocity v_y from thermally induced viscosity changes would stabilize the helical pitch at a constant value if the tangential velocity v_x of the electrophoretic ion, which is due to electromagnetic rotation of the fluid, would remain constant. Actually this velocity does depend on the buffer temperature at constant current, being inversely proportional to the viscosity of the buffer[2]:

$$v_x = (h^2/(80\eta))\,(JB), \tag{11}$$

where J and B are the magnitudes of the mutually perpendicular vectors. (Eqn. (11) is identical with eqn. (4) of ref. 2 taking $v_x = u_0$).

The helical slope is determined by the ratio (from (10) and (11)):

$$\frac{v_y}{v_x} = \left(J\frac{K'}{K''}\right)\frac{80\eta}{h^2(JB)} = \left(\frac{K'}{K''}\frac{80}{h^2B}\right)\eta, \tag{12}$$

where the last parenthesis contains temperature independent parameters. The helical pitch is thus dependent on the viscosity of the buffer in the annulus and it is necessary to maintain the temperature distribution in the annulus constant to insure stable collection of separated fractions.

On the other hand, whereas the value of the pitch of the helix depends on η and, hence, on the buffer temperature, the separation between two adjacent separated components at a given distance from the injector does not. This can be seen most simply by remembering that the motion of an ion is a combination of a circular "orbital" motion with axial migration. The orbital motion is the same for all ions confined to a given cylinder surface and the axial motion, (which is the same for all

ions on the given cylinder surface), is a combination of axial flow with electrophoretic migration resulting after a migration time τ in a displacement:

$$y = v_y \tau. \tag{13}$$

It is the latter motion which determines the axial separation between two adjacent components at the collector. Taking eqns. (5), (9) and (10) into account, we obtain from eqn. (13):

$$\Delta y = y_2 - y_1 = [(v_y)_2 - (v_y)_1]\tau = \frac{d\varphi}{dy}\tau[U_2 - U_1] = (J/\sigma)\tau\left[\frac{K_2}{\eta} - \frac{K_1}{\eta}\right] = J\tau[K_2 - K_1]/(\sigma\eta), \tag{14}$$

(were K_1, K_2 are constants defined by eqn. (5) and $(v_y)_1$, $(v_y)_2$ are the axial velocities of the two ions to be separated). In view of eqn. (8), we see that the product $(\sigma\,\eta)$ is temperature independent, which means that the separation Δy is also independent of temperature.

In actual practice, in the presence of axial flow velocity u_y superimposed upon the electromigration velocity v_y, the temperature dependence of the helical slope is determined by a ratio similar to those considered in eqns. (3) and (12). Since the axial velocity of the ions in the presence of axial streaming is $dy/dt = u_y + v_y$, the helical slope is given by the expression:

$$\frac{u_y + v_y}{u_x} = \left(\frac{dp}{dy}\Big/\frac{dp}{dx}\right) + \frac{v_y}{u_x}. \tag{15}$$

As mentioned in connection with eqn. (3), the expression in parentheses is independent of viscosity and temperature; it relates to the ratio of axial flow to tangential flow. Thus, the temperature dependence of the helical pitch diminishes as the contribution of axial streaming to the axial migration velocity of the ion increases.

Eqn. (3) has another important consequence. The coordinate z, which determines the position of a point between the inner and outer surfaces of the annulus, cancels out in the expression for u_y/u_x which determines the helical pitch. This means that, for a particle of zero electrophoretic mobility, the pitch of the helix is the same whether the streak is injected at the center of the annular gap or far off center in the combination of mutually perpendicular parabolic flows. Consequently, if the streak has a finite width, particles at the edge of the streak will have the same helical pitch as those at its center and the injected streak will have no tendency toward widening as particles migrate along its helical path, provided they have a negligible diffusion coefficient. If the diffusion rate is appreciable, the widening of the streak will be a measure of the rate of diffusion of the species of particles in the streak.

PARABOLIC DIVERGENCE

Besides diffusion, there is another mechanism which can cause the streak to increase in width progressively *even if the rate of diffusion of the particles in the streak is*

zero. Let us assume that there is neither electro-osmosis nor an instrumentally imposed axial flow. The axial migration velocity of the particles in the streak will then be exclusively due to electrophoresis. The electrophoretic velocity v_y will have the same magnitude throughout the annulus (*i.e.* for all values of z). The tangential velocity v_x, however, (assuming a parabolic distribution[2]) will be maximal ($v_x°$) at the annulus center and zero at its walls. If the injected streak were as thick as the annular gap, particles at its center would have the smallest helical pitch determined by $v_y/v_x°$ and would tend toward an infinite pitch at the walls where v_x vanishes. A streak of lesser thickness, say half that of the annular gap, would get wider from turn to turn of the helix because the helical pitch of the particles near either of its edges will have a larger value than those at its center. The streak width will thus be defined by these two limiting helices of different pitch which will progressively diverge simulating a diffusion effect. We shall refer to this effect as "parabolic divergence". To minimize this effect, the injected streak is made as thin as possible and placed well centered into the zone of maximum rotational velocity in the buffer. For a streak of finite diameter, the parabolic divergence increases with increasing streak diameter due to an increase of the helical pitch for the particles located nearest the boundaries of the annulus, the pitch of the particles in the central plane of the annulus remaining constant and forming the trailing edge of the streak. For optimal results the density and electrical conductivity of the fluid forming the streak is adjusted to be as nearly as possible equal to the corresponding values for the buffer solution.

It should be emphasized that the above assumption of parabolicity of the velocity profile for the rotational as well as the axial flow is an approximation. Actually, there are reasons for deviation from a strictly parabolic profile:

(1) There is a transverse (radial) temperature gradient in the annulus and, hence, a concomitant viscosity gradient.

(2) Another consequence of the transverse temperature gradient is a gradient of the electrical conductivity of the buffer which precludes a uniform current density throughout the cross-section of the annulus.

(3) The radius of curvature of the annulus is not infinite as compared to its width, which would be required for a strictly parabolic velocity profile.

(4) The intensity of the radial magnetic field component, which is responsible for the rotational motion of the buffer, decreases with the radial distance from the magnet axis.

Nevertheless, one can easily show experimentally that the prediction of eqn. (3) of a helical pitch independent of z is reasonably close to actual experience*. Superposition of an axial flow upon electromagnetic rotation in a cell with an annulus of 5 mm width (cooled by a room temperature bath) so as to yield a central helix of 7 mm pitch at a current of 25 mA, produced a variation in helical pitch of only about 1 mm as the injector exit was moved from the center of the annulus to a distance of about 0.5 mm of either wall. The choice of a wide annulus to increase the rate of rotation and of a low potential gradient to reduce the rate of electrophoresis created conditions approximating the assumptions underlying eqn. (3).

* This conclusion holds even in case of a non-parabolic velocity distribution of $f(z)$. Eqns. (1) and (2) then become: (1)' $u_x = f(z)\, dp/dx$ and (2)' $u_y = f(z)\, dp/dy$. Their ratio leads again to eqn. (3).

THERMAL CONVECTION

We shall deal now with the principal artifact, thermal convection. We have to distinguish between two types of thermally induced vortices: (A) those which are due to a radial temperature gradient in the annulus which maintains a flow of heat from the electrophoretic column to the coolant circulating along the outer wall and the inner wall of the annular space and (B) convection due to longitudinal temperature gradients which are parallel to the direction of axial buffer flow.

The former type of convection (A) involves vortical motion about horizontal axes which are parallel to the magnet axis. Such convections have been considered in a previous publication[4]. The second type of convection (B) is caused by temperature variation along the length of the annular electrophoretic column which arises from several causes: (a) The electrical current density in the annulus is much higher than in the buffer compartments. Hence, there is a rather sharp temperature change in the annular buffer column near the boundaries of the buffer compartments. (b) The above temperature change at the annulus–buffer compartment junction is complicated by the process of cooling the annular space. If the temperature of the coolant is much lower than the temperature in the compartments B_1, B_2 and if the electrophoretic current is not very high, there will be a negative temperature gradient (temperature drop as we enter the annulus) at the entry points of buffer into the annulus (Case I). If, on the other hand, the coolant and the buffer are at room temperature, passage of the electrophoretic current will generate a positive temperature gradient (temperature rise as we enter the annulus and proceed toward the center of the electrophoretic column) at the points of junction of the annular space with the buffer compartments (Case II). (c) In the presence of axial streaming, the temperature distribution

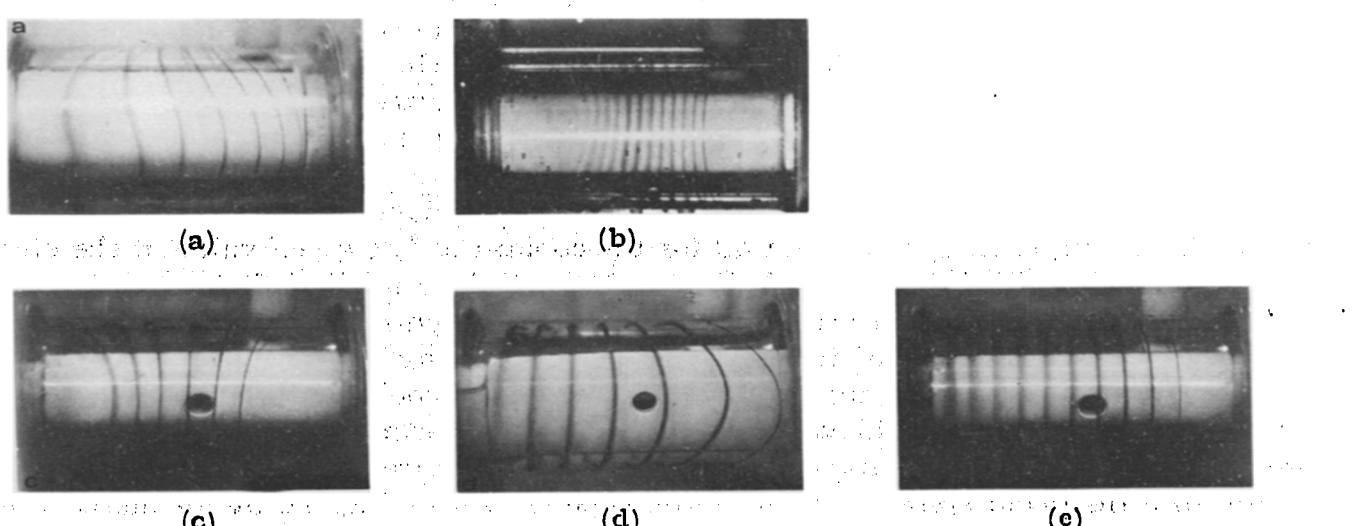

Fig. 1. Patterns of thermal convection. (a) Convection in the absence of cooling fluid. (b) Convection due to overheating of fluid column at the ends caused by partial obstruction raising the current density. (c) Distortion of helical pattern under normal conditions of cooling at a low current density. (d) Change in the type of distortion of helical pattern shown in (c) obtained by replacing cooling fluid by warm water. (e) Rectification of distorted pattern of the type shown in (c) by increasing the current.

* The photographs shown in Fig. 1 were obtained with a special demonstration cell. Cooling was accomplished by a water bath surrounding the annular electrophoretic column.

in the annular cylinder parallel to the flow is not symmetrical, the temperature being lower at the upstream end than at the downstream end.

Fig. 1a shows the distortion of the helical path due to convection engendered by longitudinal temperature gradients in the absence of cooling fluid. In order to understand such convection patterns we performed the following experiments. Fig. 1b illustrates the effect of insertion of partial obstructions into the ends of the annular column. This raises the electrical current density at the ends of the electrophoretic column. The warm buffer near the column's ends rises while the cooler buffer in the central region sinks on the side facing the reader, thus generating a counterclockwise convection on the right side and a clockwise one on the left side. The downward motion of the cooler buffer near the center is superimposed upon the downward rotational motion accelerating it and thus causing the helical streaks to move close to each other on this side of the horizontal column. On the back of the column, the conditions are reversed. On this side the downward convective motion of the buffer in the central region has the opposite direction to the upward motion which is due to electromagnetic rotation thus retarding it. This retardation is evidenced by spreading of the helical streaks on this side of the annulus. The change in the relative separation of the streaks on the opposite sides of the annular cylinder is analogous to the familiar picture of convergence of streamlines in a pattern of accelerating flow depicting transition of flow from a wide to a narrow cross section of a conduit.

A modified illustration of such convection can be obtained as follows. In Fig. 1c water at 15° is used as cooling fluid while the buffer in the buffer compartments is at room temperature. If the current is low enough, the temperature in the central region of the annular column will be lower than in the buffer compartments. As a result, the fluid will tend to descend in the central region of the horizontal fluid column and to rise near the ends of the electrophoretic column. The descent due to thermal convection accelerates the downward fluid motion caused by magnetic rotation on the side nearest the reader giving rise to the distortion of the helical pattern shown in Fig. 1c. Conversely, if we use warm water, 45°, as "coolant," we obtain a spreading of the helical turns as shown in Fig. 1d due to a reversed convection pattern*.

Comparison between Figs. 1c and 1d makes the conclusion plausible that an intermediate temperature can be found for the coolant at the given value of the electrophoretic current for which the helical pattern is intermediate between the two distorted patterns shown in these figures and which is symmetrical having the same distance between the turns of the helix on the side facing the reader as on the opposite side. Instead of changing the temperature of the coolant to achieve this symmetrical pattern, one can achieve the same result by altering the temperature of the annular buffer column by changing the electrophoretic current. Fig. 1e shows a rectification of a distorted spiral pattern of the type shown in Fig. 1c by an increase in current. For a given temperature of the coolant there is an optimum electrophoretic current value at which convective distortions like those described above are minimized.

* The asymmetry of the convection pattern in Fig. 1d is very instructive. It is due to the fact that the left buffer compartment in the apparatus used was much smaller than the right one. As a result, the temperature in the left buffer compartment rose appreciably above that in the right compartment in the course of experiments thus minimizing the temperature difference between the annulus and buffer compartment at the left end of the annulus, which resulted in almost complete suppression of convection.

RESOLVING POWER

In considering the resolving power of the instrument, we must distinguish between resolution in the separation pattern and resolution in the collection pattern. We shall consider the former resolving power at first. The maximum resolution will be achieved in the absence of diffusion. Thus, the method is most favorable for separation of macromolecules or suspended microscopic particles, where there is no perceptible widening of the streak due to diffusion. There will be, however, a streak widening due to "parabolic divergence". This limitation can be minimized by good centering of the streak in the velocity profile and by making the streak as thin as possible.

We shall now consider quantitatively the limitation of resolving power by parabolic divergence. We shall set up a criterion for the limit of resolution and derive an equation determining the maximum width of the injector which can be used to resolve two components of a given mobility difference.

For ease of visualization and representation, we imagine the cylindrical surfaces of the annular cylinder rolled out over a flat surface so that the axial flow direction is parallel to the y axis and the direction of tangential flow (due to fluid rotation) is parallel to the x-axis as shown in Fig. 2a. The z-axis is perpendicular to the plane of the paper. It corresponds to the radial dimensions of the original annulus whose thickness is h. The coordinate z measures the distance of a point from one of the two planes sandwiching between them the rectified annular buffer column (namely, from the plane obtained by flattening the inner cylinder) whereas the distance of the same point from the flattened outer cylinder plane is given by $(h-z)$.

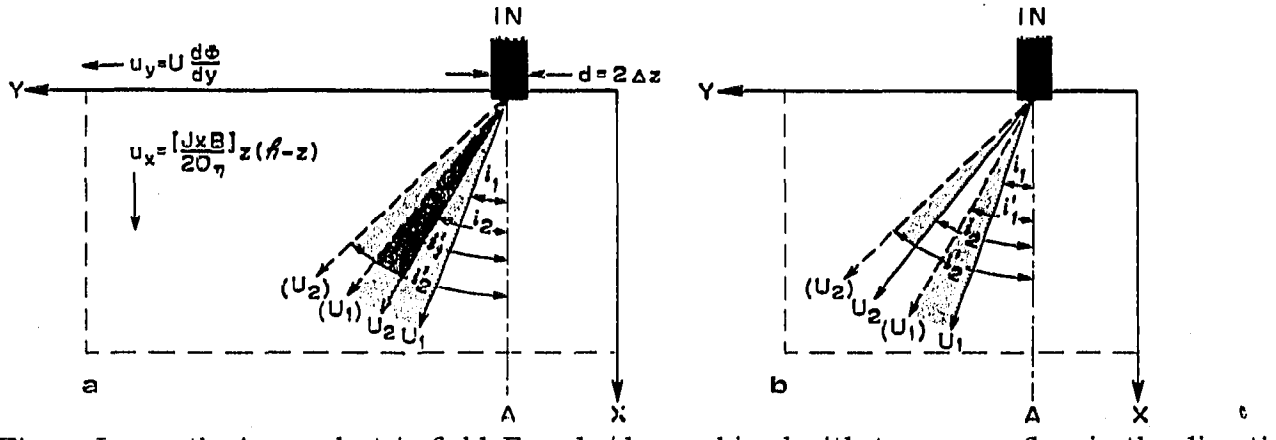

Fig. 2. Ion paths in an electric field $E = d\varphi/dy$ combined with transverse flow in the direction of the X-axis. u_y: velocity due to electrophoresis. u_x: fluid flow velocity. Solid line trailing edge, dashed line leading edge of an ion streak IN = Injector.

The helical paths of the ions are now replaced by straight lines inclined by the angles i against the axis A which represents the path of an uncharged particle.

We should keep in mind that the ion velocity u_y is entirely due to electromigration and is independent of z. Its value throughout the cross-section of the annulus is given by:

$$u_y = U\frac{d\varphi}{dy}. \qquad (15)$$

The velocity u_x, on the other hand, is imposed upon the ions by fluid rotation and is subject to the parabolic velocity distribution which prevails in the tangential laminar flow. As shown previously (eqns. (2) and (3) of ref. 2),:

$$u_x = \frac{(JB)}{2o\eta} z(h - z). \tag{16}$$

For the special case of a particle located in the central layer of the annulus ($z = h/2$) we obtain the velocity:

$$(u_x)_0 = \frac{(JB)}{8o\eta} h^2. \tag{17}$$

Another case which is of interest to us, is a particle located in a layer which deviates from the coordinate $h/2$ of the central layer by a small amount Δz. We shall designate the value of u_x in this layer by $(u_x)_{\Delta z}$. We obtain the expression for $(u_x)_{\Delta z}$ by setting $z = h/2 + \Delta z$ in eqn. (16). We obtain thus:

$$(u_x)_{\Delta z} = \frac{(JB)}{2o\eta}\left(\frac{h}{2} + \Delta z\right)\left(h - \frac{h}{2} - \Delta z\right) = \frac{(JB)}{2o\eta}\left[\left(\frac{h}{2}\right)^2 - (\Delta z)^2\right] \tag{18}$$

Remembering the expression for the central velocity u_0 given in eqn. (17), we can replace in eqn. (18) the factor $(JB/2o\,\eta$ by $4\,[(u_x)_0/h^2]$.

We obtain thus:

$$(u_x)_{\Delta z} = (u_x)_0\left[1 - \left(\frac{2\Delta z}{h}\right)^2\right]. \tag{18a}$$

In view of the fact that half the thickness $d/2$ of an injector represents the maximum deviation Δz of a particle path in the injected streak from the streak center (which is normally adjusted to coincide with the center of the velocity profile), we can substitute in eqn. (18a) $2\,\Delta z$ by d. We obtain thus:

$$(u_x)_{\Delta z} = (u_x)_0\left[1 - \left(\frac{d}{h}\right)^2\right]. \tag{18b}$$

We can now return to Fig. 2 to consider the problem of the resolution of two adjacent streaks corresponding to components of mobilities U_1 and $U_2 > U_1$. If the injector were infinitely thin ($d = 0$) we would have only two streaks of mobilities U_1 and U_2 forming the angies i_1 and i_2 with the A axis (we assume the injector to be well centered in the velocity distribution of the fluid flow traversing the annulus). Actually, due to the finite thickness d of the injector along the direction of the z-axis, the streaming velocity u_x is lowest for the ions leaving the injector near those points of its periphery which are closest to the walls of the annulus. It is highest at the injector center which coincides with the maximum of the parabolic velocity distribution of u_x. This means that the ions leaving the injector near the streak periphery close to the aforementioned points will be deviated by a larger angle i' than those at

the center of the streak, which proceed at the angle i. The angle i follows from the expression for the slope of a particle path:

$$\tan i = \frac{u_y}{u_x}. \tag{19}$$

We thus have for the particles moving along the centers of two streaks corresponding to components of mobilities U_1 and U_2:

$$\tan i_1 = \frac{(u_y)_1}{(u_x)_0} \tag{20a}$$

$$\tan i_2 = \frac{(u_y)_2}{(u_x)_0} \tag{20b}$$

and for particles emanating from the proximal or distal points of the injector periphery as viewed by the reader in Fig. 2a:

$$\tan i'_1 = \frac{(u_y)_1}{(u_x)_{\Delta z}} \tag{21a}$$

$$\tan i'_2 = \frac{(u_y)_2}{(u_x)_{\Delta z}}. \tag{21b}$$

Δz In above equation is equal to the injector radius and $(u_x)_{\Delta z}$ stands for the tangential velocity component due to electromagnetic propulsion at a point removed from the central maximum of the velocity distribution by the distance Δz.

The leading edges (U_1) and (U_2) of the streaks are shown originating at the same point as their trailing edges U_2 and U_1 in Fig. 2a. Actually, their points of origin do not coincide in space but only appear to coincide in projection as viewed by the reader. The trailing edges U_1 and U_2 are traced by particles of both components originating at the injector's center. The leading edges (U_1) and (U_2) are traced by particles originating at points of the injector periphery which lie exactly above or below the injector center as viewed by the reader. The angular deviations of the streak edges (U_2) and (U_1) are larger than those of U_2 and U_1 because the velocities due to electromagnetic streaming $(u_x)_{\Delta z}$ are smaller at the points of origin of the leading edges (U_1) and (U_2) than the central velocity $(u_x)_0$ which prevails at the point of origin of the trailing edges U_1 and U_2. In Fig. 2 U_1, and (U_1) are thus the trailing and the leading edge of the streak of the electrophoretically slower component and U_2 and (U_2) those of the faster component. We see from Fig. 2a that each streak diverges, the angle of divergence being given for the mobility U_1 by $(i_1' - i_1)$ and for the mobility U_2 by $(i_2' - i_2)$. The two streaks are seen to overlap in Fig. 2a. The region between the lines labeled U_2 and (U_1) contains ions of both species. Fig. 2b shows, on the other hand, a complete separation of components bearing the same labels. It is clear from these diagrams that the limiting case of adequate resolution without overlap is given by the condition for coincidence of the leading edge of the slower component (U_1) with the trailing edge U_2 of the faster component, in which case:

$$i'_1 = i_2. \tag{22}$$

Taking advantage of our eqns. (20), (21) and (22) we write:

$$\tan i_1' = \tan i_2, \tag{22a}$$

from which follows:

$$\frac{(u_y)_1}{(u_x)_{\Delta z}} = \frac{(u_y)_2}{(u_x)_0} \tag{23}$$

Substituting in eqn. (23) the values given for Δu_y and $(u_x)_{\Delta z}$ in eqns. (15) and (18b) we obtain:

$$\frac{U_1 \frac{d\varphi}{dy}}{(u_x)_0 \left[1 - \left(\frac{d}{h}\right)^2\right]} = \frac{U_2 \frac{d\varphi}{dy}}{(u_x)_0} \tag{24}$$

Solving for the width of the injector d we obtain:

$$d^2 = h^2 \frac{(U_2 - U_1)}{U_2} \tag{25}$$

Setting $U_2 - U_1 = \Delta U$ we obtain the desired equation which determines the maximum width d which we can choose for an injector if we wish to resolve components of mobilities U_1 and U_2 differing by ΔU:

$$d = h \sqrt{\frac{\Delta U}{U_2}} \tag{25a}$$

Let us consider a numerical example. The mobility of the faster ion is U_2. Let us assume that the slower component U_1 differs from the faster one by 1 % so that $\Delta U = 10^{-2}\, U_2$ and we assume $h = 2 \cdot 10^{-1}$ cm. We obtain then for the maximum usable injector diameter:

$$d = 2 \cdot 10^{-1} \sqrt{\frac{10^{-2} U_2}{U_2}} = 2 \cdot 10^{-2} \text{ cm} = 0.2 \text{ mm}$$

This is the order of magnitude of the inside diameter of the hypodermic needles normally used as injectors.

We see that the separation scale can be increased by increasing the injector diameter d only at a sacrifice of resolving power. The larger the ratio $\Delta U/U_2$ for the mobilities of the components to be separated, the easier it is to achieve a large-scale separation because of the larger permissible value of d. On the other hand, for maximum resolution, one could use injector diameters of microscopic dimensions.

We can take as a measure of the resolving power R of the apparatus the reciprocal of the relative mobility difference $\Delta U/U_2$ which will give rise to two non-overlapping streaks:

$$R = \frac{U_2}{\Delta U} = \left(\frac{h}{d}\right)^2. \tag{26}$$

We see that the resolving power increases quadratically with the ratio of the width of the annular gap to the internal injector diameter.

These considerations concerning the resolving powers are not limited to the magnetically stabilized rotational electrophoresis apparatus. They apply equally well to the serpentine electrophoresis method and even more strictly to fluid curtain methods of deviation electrophoresis.

SUMMARY

Temperature gradients engendered in the annular electrophoretic column can lead to disturbing thermal convection. Different types of convection and means to suppress such disturbances are discussed. Effects of temperature on the separation pattern are considered and an equation is derived for the resolving power of the separation method which is generally valid for all methods of deviation electrophoresis. It is shown that separation of two components differing 1 % in their electrophoretic mobilities presents no difficulties and a basis is provided for the inference that higher resolving power can be reached by using exceedingly fine streaks.

REFERENCES

1 A. KOLIN, *J. Chromatog.*, 26 (1967) 164.
2 A. KOLIN, *Proc. Natl. Acad. Sci. U.S.A.*, 46 (1960) 509.
3 H. LAMB, *Hydrodynamics*, Dover, New York, 1945, p. 582.
4 A. KOLIN, *Proc. Natl. Acad. Sci. U.S.A.*, 51 (1964) 1110.
5 G. JOOS, *Theoretical Physics*, Harper, New York, 1950, p. 419.